Overview on Low Temperature Co-fired Ceramic Sensors

Supplement: sensitivity of piezoresistive pressure sensor

This supplement provides background information on the calculated vs. measured raw bridge sensitivity of the pressure sensor [S1] described in Section 3.1.2 (Figures 14 and 15) of the main paper, or the identical pressure-sensing part of the integrated pressure / flow / temperature compressed-air sensor [S2] described in Section 3.6 (Figures 38 and 39). In these studies [S1, S2], as the pressure sensor was fitted with an integrated bridge-conditioning circuit, no information on the raw, unamplified response of the piezoresistive bridge was available. This response was later measured on identical membranes (Table S1, Figure S1) in the frame of a Masters project [S3].

Here, we compare the experimental results with calculations using published data on the LTCC substrate and the piezoresistors, and arrive at reasonably close agreement. We then successfully extend this comparison to the other piezoresistive sensor described in Section 3.1.2 (Figures 12 and 13).

Thereby, we also establish the relation between the "usual" gauge factors, determined by cantilever bending tests, and the more general "planar" ones that can be applied to any in-plane strain configuration such as membrane pressure sensors.

Table S1. Parameters of the LTCC pressure-sensing cell (see Figure S1).

Parameter	Symbol	Value
LTCC material		DuPont 951
Resistor material		DuPont 2041 (10 kΩ nominal)
Firing		Co-firing, 30 min at 850-875°C
Membrane thickness	h	95, 138 and 212 µm (fired)[1]
Membrane radius	R	1.80 mm
Resistor radial position, centre	r^+	0.45 mm
Resistor radial position, edge	r^-	1.60 mm
Resistor length (parallel to current)	L_R	0.40 mm
Resistor width (perpendicular to current)	b_R	0.50 mm

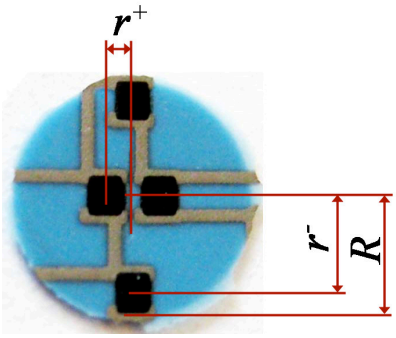

Figure S1. Pressure sensor membrane (piece broken off during overpressure tests [S3]), with depicted membrane radius R and resistor radial positions r^+ and r^-.

[1] Unfired LTCC thickness is 114, 165 and 254 µm; fired thickness calculated with assumed 16.6% out-of-plane shrinkage, see table S2.

Membrane deformation and piezoresistor response

On the sensing surface of a circular membrane, the ideal radial (ε_r) and tangential (ε_t) strains resulting from application of a differential pressure ΔP (sign: positive = overpressure opposite the sensing surface) may be calculated with the following relations [S5]:

$$\varepsilon_r(r) = \frac{3\cdot(1-\nu^2)}{8E\cdot h^2}\cdot\left(R^2-3r^2\right)\cdot\Delta P \quad (1)$$

$$\varepsilon_t(r) = \frac{3\cdot(1-\nu^2)}{8E\cdot h^2}\cdot\left(R^2-r^2\right)\cdot\Delta P \quad (2)$$

ε_r	radial strain at surface
ε_t	tangential strain at surface
ΔP	applied differential pressure
R	LTCC membrane radius
h	LTCC membrane thickness
r	distance from centre of membrane
E	LTCC Young's modulus
ν	LTCC Poisson's coefficient

Assuming that the resistors are sufficiently small with respect to the membrane, we can calculate the response of "radial" (current flowing radially, z_r) and "tangential" (current flowing tangentially, z_t) resistors, taking r to be the radial position of their centre of gravity and using the "planar" gauge factors, J_L and J_T:

$$z_r(r) = J_L\cdot\varepsilon_r(r) + J_T\cdot\varepsilon_t(r) \quad (3)$$

$$z_t(r) = J_L\cdot\varepsilon_t(r) + J_T\cdot\varepsilon_r(r) \quad (4)$$

z_r	response of "radial" resistors
z_t	response of "tangential" resistors
J_L	"planar" longitudinal gauge factor
J_T	"planar" transverse gauge factor
r	radial position (centre of resistor)

Relationship between gauge factors

It must be mentioned that these "planar" gauge factors, J_L and J_T, are defined for a single in-plane strain (with out-of-plane deformation remaining free), and therefore do not correspond to the "usual" ones obtained from cantilever bending tests, GF_L, and GF_T. While more extended mathematical treatment may be used to obtain the fundamental piezoresistive coefficients [S6, S7], one may simply correlate both sets of gauge factors using their respective boundary condition: single in-plane strain for the "planar" ones, vs., for the "usual" ones, in-plane strains linked by the substrate Poisson coefficient. Therefore, we obtain GF_L, and GF_T through simple strain superposition:

$$GF_L = J_L - J_T\cdot\nu \quad (5)$$

$$GF_T = J_T - J_L\cdot\nu \quad (6)$$

GF_L	"usual" longitudinal gauge factor
GF_T	"usual" transverse gauge factor

Conversely, as we rather usually know the other pair, GF_L and GF_T, we rearrange (5) and (6) accordingly to calculate J_L, and J_T:

$$J_L\cdot\left(1-\nu^2\right) = GF_L + GF_T\cdot\nu \quad (7)$$

$$J_T\cdot\left(1-\nu^2\right) = GF_T + GF_L\cdot\nu \quad (8)$$

Mechanical strains and derived piezoresistive response - example

An example plot of the strains, calculated using (1) and (2) as a function of the radial position r (= distance from the centre) is given in Figure S2, for a pressure of 0.1 MPa (1 bar). Using (3) and (4) and the planar gauge factors calculated with (7) and (8), the resulting resistor responses are given in Figure S3. This example corresponds to our actual sensor (midrange membrane thickness).

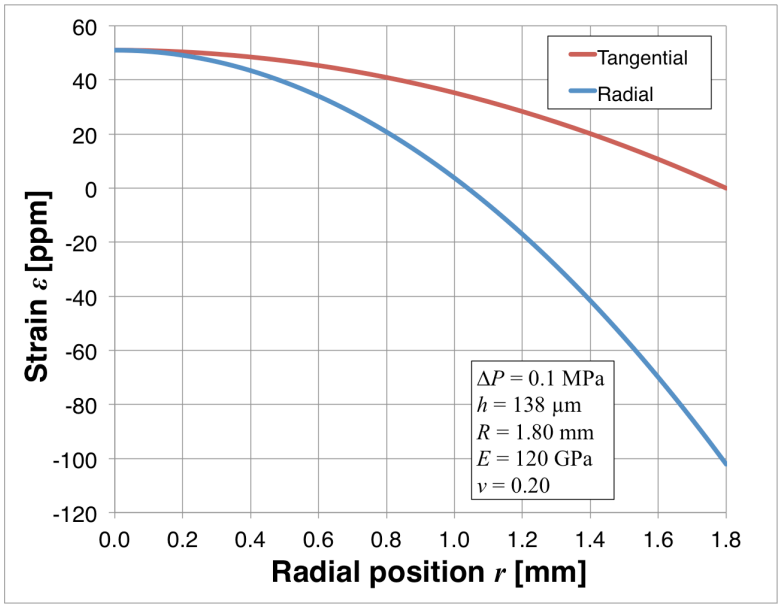

Figure S2. Plot of ideal radial (ε_r) and longitudinal (ε_t) strains on LTCC membrane surface, for parameters indicated in inset (ppm = parts per million, i.e. 10^{-6}).

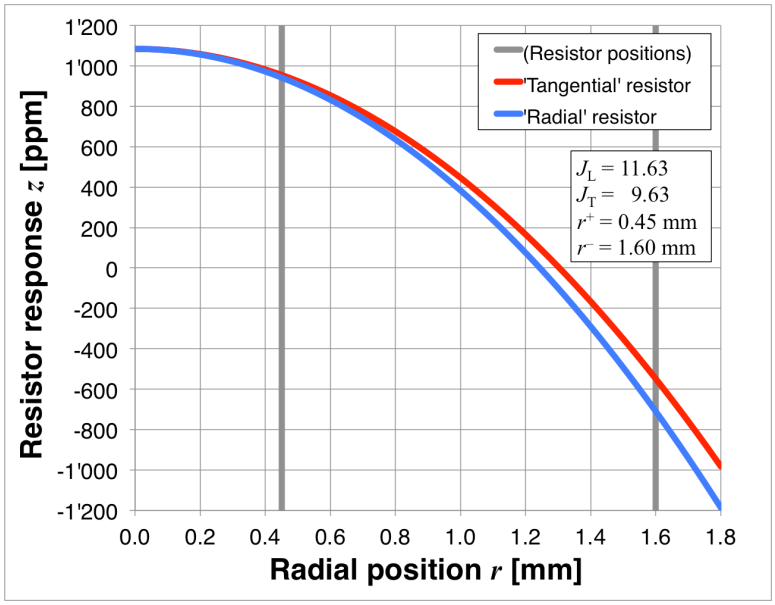

Figure S3. Calculated responses of "radial" (z_r) and "tangential" (z_t) resistors, from the strains given in Figure S2 and using the parameters indicated in inset. Radial position of resistors for our actual sensor (see Table S1) indicated by vertical grey lines.

Arrangement and placement of the sensing resistors

Several salient features may be noticed in the plots of Figures S2 and S3, which have implications on sensor design (see e.g. Figure S1):

- **At the centre**, the radial and tangential strains are equal and have zero derivative with *r*, i.e. placement of the central resistors is not very critical. As the radial strain decreases faster than the tangential one and resistor longitudinal gauge factors are larger than transverse ones, it is slightly more advantageous to use a lozenge configuration than an in-line one (see Figure S4), i.e. with "tangential" central resistors rather than "radial" ones, except possibly if the resistors are very short.
- **At the edge**, placement of the opposite resistor pair is more critical than at the centre, and resistors must be sufficiently short with respect to the membrane size, so as not to lose too much signal (Figure S3). As tangential stress goes to zero and given the relationship between the gauge factors, resistors should have a "radial" orientation.

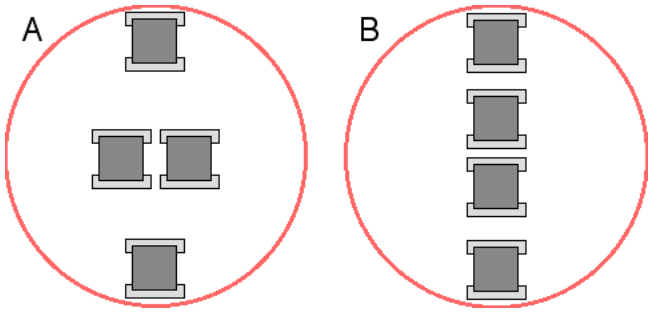

Figure S4. Possible resistor configurations on membrane: A) lozenge, with "tangential" central resistors; B) in-line, with "radial" central resistors.

Reported properties of DuPont 951 LTCC and 2041 piezoresistors

Reported values of the elastic modulus E and firing shrinkage of DuPont LTCC, for work where processing conditions were specified, are given in Table S2. Reported values of E are close to supplier indications [S8], and lie mostly in the 110…125 GPa range, with $E = 120$ GPa retained for our calculations. Some discrepancies are normal, given the process-dependent density and phase composition of the material [S9].

No explicitly-measured values of the Poisson coefficient have been found (a parameter that has less influence than E and that may be measured e.g. using ultrasound techniques [S10]). with assumed values lying between 0.17 and 0.22 (see also discussion in [S11]). We therefore retain $\nu = 0.20$.

Membrane thickness was determined from green thickness by applying the out-of-plane shrinkage that we determined from similar samples with free-standing structures [S13], 16.6%. Out-of-plane firing shrinkage is specified by the supplier to be 15.0% ± 0.5% [S8], which applies to the indicated processing conditions (lamination at 21 MPa, 70°C). Actual shrinkage depends on process conditions, and is expected to be somewhat larger for our membranes, in agreement with our measurements, as they lie atop a cavity and therefore do not experience the lamination pressure.

Gauge factors determined for DuPont 2041 fired atop 951 LTCC are given in Table S3. The rather strong variability is expected, given the variability of fabrication conditions (post-firing, co-firing, firing schedule, resistor thickness), which affect the resistor material both directly (firing schedule) and through resistor-LTCC interactions (all parameters). We retain here the values determined from cantilever bending experiments [S14], which lie in the midrange of reported values, and use them to calculate the "planar" gauge factors J_L and J_T.

Table S2. Reported properties of DuPont 951 LTCC.

Processing conditions & reference	**Young's modulus *E*** [GPa]	**Poisson coefficient *v*** (assumed)	**Out-of-plane (z) firing shrinkage**
Indicated by supplier [S8]	120		15.0%
Fired 850°C, 15 min [S9]	122	-	-
Fired 875°C, 15 min [S9]	120	-	-
Fired 850°C, 20 min [S11]	115	0.17…0.22	-
Fired 850°C [S12]	110	-	-
Fired 880°C, 30 min [S13], free-standing†	-	-	16.6%
Laminated, dilatometry to ~950°C [S15]	-	-	17.0%
Values retained in this work	**120**	**0.20**	**16.6%**

† Determined on free-standing structure, which did not experience the lamination pressure.

Table S3. Reported gauge factors determined for DuPont 2041 resistors.

Processing conditions & reference	**Longitudinal GF_L**	**Transverse GF_T**
Unspecified, presumably 850°C [S7]		
- Co-fired on DuPont 951	7.9	5.2
- Post-fired on DuPont 951	8.2	5.6
Fired at 850°C [S12]		
- Co-fired on DuPont 951	9.9	-
- Post-fired on DuPont 951	9.6	-
Co-fired on DuPont 951, 850…875°C [S14]†	9.7	7.3
Co-fired on DuPont 951, 850°C [S16]	12.5	-
Post-fired on DuPont 951, 850°C [S17]	12.5	-
Retained values [S13]	**9.7**	**7.3**
Planar gauge factors, calculated using (7) and (8)	J_L **= 11.63**	J_T **= 9.63**

† Initially determined with incorrect elastic modulus; recalculated with retained values of *E* and *v* for fired DuPont 951.

Sensor response: comparison of calculated and measured values

From the data of the pressure-measurement cells (Table S1 for ø3.6 mm membrane, [S4] for ø9.6 mm one) and the retained gauge factors, we calculate the response of the piezoresistors. The central piezoresistors have a "tangential" orientation, so we apply (3) to calculate their response z^+:

$$(9) \quad z^+ = J_L \cdot \varepsilon_t\left(r^+\right) + J_T \cdot \varepsilon_r\left(r^+\right)$$

Conversely, we apply (4) to obtain the response z^- of the "radial" resistors at the edge:

$$(10) \quad z^- = J_L \cdot \varepsilon_r\left(r^-\right) + J_T \cdot \varepsilon_t\left(r^-\right)$$

The calculated bridge response z_{calc} is simply the differential one:

$$(11) \quad z_{calc} = z^+ - z^-$$

Calculated responses z_{calc}, for applying $\Delta P = 100$ kPa on the ø3.6 mm membrane and $\Delta P = 10$ kPa on the ø9.6 mm one, are given in Table S4, and compared with measured ones z_{exp} [S3, S4], scaled to the respective pressure. Reasonable agreement is obtained in all cases, given the many uncertainties: membrane stress, thickness, flatness and clamping, and resistor gauge factors. For very thin membranes, deviations from flatness and internal stress are the main issues, with the effect of films (e.g. resistors and overglaze) on the mechanical behaviour also becoming non-negligible. For thicker membranes, good clamping becomes more critical, with strain at the edges deviating from ideal membrane theory; finite-element modelling (FEM) therefore must be used to obtain more accurate values.

Table S4. Comparison of calculated and measured pressure cell response.

Sensor type (membrane diameter)	*2R*	**3.6†**	**3.6†**	**3.6†**	**9.6***	mm
Membrane thickness	h	95	138	212	100	µm
Applied pressure	ΔP	100	100	100	10	kPa
Calculated response - Central resistors - Edge resistors	 z^+ z^-	 +2'014 –1'496	 +961 –714	 +406 –301	 +1'470 –1'010	 ppm (µV/V)
Calculated bridge response	z_{calc}	1'755	838	354	1'240	ppm (µV/V)
Measured bridge response	z_{exp}	2'010	798	321	1'400	ppm (µV/V)
Difference, calculated vs. measured		–13%	+5%	+10%	-11%	

† 3.6 mm diameter membrane corresponds to sensor whose data is given in Table S1.

* 9.6 mm diameter membrane corresponds to the other pressure sensor in this review [S4]

References

[S1] Y. Fournier, A. Barras, G. Boutinard Rouelle, T. Maeder, P. Ryser, SMD pressure and flow sensors for industrial compressed air in LTCC technology, in: Proceedings of 17th European Microelectronics & Packaging Conference (EMPC), Rimini, Italy, 2009.

[S2] Y. Fournier, T. Maeder, G. Boutinard Rouelle, A. Barras, N. Craquelin, P. Ryser, Integrated LTCC pressure / flow / temperature multisensor for compressed air diagnostics, Sensors 10 (2010) 11156-11173.

[S3] J.-B. Coma, *Caractérisation d'un capteur industriel d'air comprimé* [characterisation of an industrial compressed-air sensor], Masters Project, *Laboratoire de Production Microtechnique*, EPFL, Lausanne, Switzerland, 2010.

[S4] M. Santo Zarnik, D. Belavič, Study of LTCC-based pressure sensors in water, Sensors and Actuators A 199 (2013) 334-343.

[S5] W.K. Schomburg, Strain gauges on membranes, in: Introduction to Microsystem Design, RWTHedition, Springer, Berlin, Germany, 53-64, 2011.

[S6] M. Santo Zarnik, D. Belavič, K.P. Friedel, A. Wymysłowski, A procedure for validating the finite element model of a piezoresistive ceramic pressure sensor, IEEE Transactions on Components and Packaging Technologies 27 (2004) 668-675.

[S7] M. Santo Zarnik, D. Belavič, A. Wymysłowski, Evaluation of gauge coefficients for modelling piezoresistive properties of thick-film resistors, Sensors and Materials 18 (2006) 261-275.

[S8] 951 Green Tape™, technical datasheet, DuPont Microcircuit Materials (USA), 2003.

[S9] K. Makarovič, R. Bermejo, I. Kraleva, A. Benčan, M. Hrovat, J. Holc, B. Malič, M. Kosec, The effect of phase composition on mechanical properties of LTCC material, International Journal of Applied Ceramic Technology 10 (2013) 449-457.

[S10] J.-D. Aussel, J.-P. Monchalin, Precision laser-ultrasonic velocity measurement and elastic constant determination, Ultrasonics 27 (2004) 165-177.

[S11] Y.F. Zhang, S.L. Bai, M. Miao, Y.F. Jin, Microstructure and mechanical properties of an alumina–glass low temperature co-fired ceramic, Journal of the European Ceramic Society 29 (2009) 1077-1082.

[S12] D. Belavič, M. Hrovat, M. Santo Zarnik, J. Cilenšek, J. Kita, L. Golonka, A. Dziedzic, W. Smetana, H. Homolka, R. Reicher, Benchmarking different substrates for thick-film sensors of mechanical quantities, in: Proceedings of the 15th European Microelectronics and Packaging Conference (EMPC), Bruges, Belgium, 216-221, 2005.

[S13] Y. Fournier, R. Willigens, T. Maeder, P. Ryser, Integrated LTCC micro-fluidic modules - an SMT flow sensor, in: Proceedings of the 15th European Microelectronics and Packaging Conference (EMPC), Bruges, Belgium, 577-581, 2005.

[S14] M. Boers, *Micro-cellules de force en technologie LTCC* [Micro force cells in LTCC technology], Semester project, *Laboratoire de Production Microtechnique*, EPFL, Lausanne, Switzerland, 2005.

[S15] C.B. DiAntonio, D.N. Bencoe, K.G. Ewsuk, Characterization and control of low temperature co-fire ceramic (LTCC) processing, in: Proceedings, Ceramic Interconnect Technology Conference, Denver, USA, 160-164, 2003.

[S16] D. Belavič, M. Hrovat, A. Dziedzic, L. Golonka, J. Kita, J. Holc, S. Drnovšek, M. Kosec, M. Santo Zarnik, An investigation of thick-film materials for sensors and actuators, in: Proceedings, XXIX International Conference of IMAPS Poland, Koszalin-Darłówko, 357-360, 2005.

[S17] M. Hrovat, D. Belavič, A. Benčan, J. Bernard, J. Holc, J. Cilenšek, W. Smetana, H. Homolka, R. Reicher, L. Golonka, A. Dziedzic, K. Kita, Thick-film resistors on various substrates as sensing elements for strain-gauge applications, Sensors and Actuators A 107 (2003) 261-272.